Original Article

Baseline radiologic features as predictors of efficacy in patients with pancreatic neuroendocrine tumors with liver metastases receiving surufatinib

Jianwei Zhang[1*], Haibin Zhu[2*], Lin Shen[3], Jie Li[1], Xiaoyan Zhang[2], Chunmei Bai[4], Zhiwei Zhou[5], Xianrui Yu[6], Zhiping Li[7], Enxiao Li[8], Xianglin Yuan[9], Wenhui Lou[10], Yihebali Chi[11], Nong Xu[12], Yongmei Yin[13], Yuxian Bai[14], Tao Zhang[15], Dianrong Xiu[16], Jia Chen[17], Shukui Qin[18], Xiuwen Wang[19], Yujie Yang[20], Haoyun Shi[20], Xian Luo[20], Songhua Fan[20], Weiguo Su[20], Ming Lu[3], Jianming Xu[21]

[1]Key Laboratory of Carcinogenesis and Translational Research (Ministry of Education/Beijing), Department of Gastrointestinal Oncology, Peking University Cancer Hospital & Institute, Beijing 100142, China; [2]Key Laboratory of Carcinogenesis and Translational Research (Ministry of Education/Beijing), Department of Radiology, Peking University Cancer Hospital & Institute, Beijing 100142, China; [3]State Key Laboratory of Holistic Integrative Management of Gastrointestinal Cancers, Beijing Key Laboratory of Carcinogenesis and Translational Research, Department of Gastrointestinal Oncology, Peking University Cancer Hospital & Institute, Beijing 100142, China; [4]Department of Medical Oncology, Peking Union Medical College Hospital, Chinese Academy of Medical Sciences and Peking Union Medical College, Beijing 100730, China; [5]Department of Gastric Surgery, State Key Laboratory of Oncology in South China, Collaborative Innovation Centre for Cancer Medicine, Sun Yat-sen University Cancer Center, Guangzhou 510062, China; [6]Department of Pancreatic and Hepatobiliary Surgery, Fudan University Shanghai Cancer Center, Shanghai 200032, China; [7]Department of Abdominal Oncology, West China Hospital, Sichuan University, Chengdu 332001, China; [8]Department of Medical Oncology, the First Affiliated Hospital of Xi'an Jiaotong University, Xi'an 710061, China; [9]Department of Oncology, Tongji Hospital, Tongji Medical College, Huazhong University of Science and Technology, Wuhan 430030, China; [10]Department of General Surgery, Zhongshan Hospital of Fudan University, Shanghai 200032, China; [11]Department of Medical Oncology, National Cancer Center/Cancer Hospital, Chinese Academy of Medical Sciences and Peking Union Medical College, Beijing 100021, China; [12]Department of Medical Oncology, the First Affiliated Hospital of Zhejiang University, Hangzhou 310009, China; [13]Department of Medical Oncology, the First Affiliated Hospital of Nanjing Medical University, Nanjing 210029, China; [14]Department of Gastrointestinal Oncology, Harbin Medical University Cancer Hospital, Harbin 150081, China; [15]Department of Oncology, Union Hospital, Tongji Medical College, Huazhong University of Science and Technology, Wuhan 430022, China; [16]Department of General Surgery, Peking University Third Hospital, Beijing 100191, China; [17]Department of Medical Oncology, Jiangsu Cancer Hospital, Nanjing 214206, China; [18]Cancer Center of Jinling Hospital, Nanjing University of Chinese Medicine, Nanjing 210016, China; [19]Department of Medical Oncology, Qilu Hospital of Shandong University, Jinan 250012, China; [20]Department of Clinical and Regulatory Affairs, HUTCHMED Limited, Shanghai 200001, China; [21]Department of Gastrointestinal Oncology, the Fifth Medical Center, Chinese PLA General Hospital, Beijing 100071, China

*These authors contributed equally to this work.

Correspondence to: Prof. Ming Lu, MD. State Key Laboratory of Holistic Integrative Management of Gastrointestinal Cancers, Beijing Key Laboratory of Carcinogenesis and Translational Research, Department of Gastrointestinal Oncology, Peking University Cancer Hospital & Institute, Beijing 100142, China. Email: qiminglu@126.com; Prof. Jianming Xu, MD. Department of Gastrointestinal Oncology, the Fifth Medical Center, Chinese PLA General Hospital, Beijing 100071, China. Email: Jmxu2003@163.com.

Abstract

Objective: Currently, pre-treatment prediction of patients with pancreatic neuroendocrine tumors with liver metastases (PNELM) receiving surufatinib treatment was unsatisfying. Our objective was to examine the association between radiological characteristics and efficacy/prognosis.

Methods: We enrolled patients with liver metastases in the phase III, SANET-p trial (NCT02589821) and obtained contrast-enhanced computed tomography (CECT) images. Qualitative and quantitative parameters including hepatic tumor margins, lesion volumes, enhancement pattern, localization types, and enhancement ratios were evaluated. The progression-free survival (PFS) and hazard ratio (HR) were calculated using Cox's proportional hazard model. Efficacy was analyzed by logistic-regression models.

Results: Among 152 patients who had baseline CECT assessments and were included in this analysis, the surufatinib group showed statistically superior efficacy in terms of median PFS compared to placebo across various qualitative and quantitative parameters. In the multivariable analysis of patients receiving surufatinib (N=100), those with higher arterial phase standardized enhancement ratio-peri-lesion (ASER-peri) exhibited longer PFS [HR=0.039; 95% confidence interval (95% CI): 0.003–0.483; P=0.012]. Furthermore, patients with a high enhancement pattern experienced an improvement in the objective response ratio [31.3% *vs.* 14.7%, odds ratio (OR)=3.488; 95% CI: 1.024–11.875; P=0.046], and well-defined tumor margins were associated with a higher disease control rate (DCR) (89.3% *vs.* 68.2%, OR=4.535; 95% CI: 1.285–16.011; P=0.019) compared to poorly-defined margins.

Conclusions: These pre-treatment radiological features, namely high ASER-peri, high enhancement pattern, and well-defined tumor margins, have the potential to serve as predictive markers of efficacy in patients with PNELM receiving surufatinib.

Keywords: Neuroendocrine tumors; liver metastases; computed tomography; surufatinib

Submitted Jul 24, 2023. Accepted for publication Sep 15, 2023.
doi: 10.21147/j.issn.1000-9604.2023.05.09
View this article at: https://doi.org/10.21147/j.issn.1000-9604.2023.05.09

Introduction

The pancreas is one of the most common primary sites among gastroenteropancreatic neuroendocrine tumors (NET) (1). Among all metastatic sites in pancreatic NETs, pancreatic neuroendocrine tumors with liver metastases (PNELM) are most commonly seen, with a prevalence of 82% in registries and 64% in the SEER database in United States (1). Liver metastases (LM) are associated with poor prognosis and a 5-year survival of 13%–54% compared to 75%–99% without LM (2,3). The European Neuroendocrine Tumor Society consensus guidelines suggest that over 80% of PNELM can only be treated systemically (4-7). PNELM are usually accompanied by abundant blood supply, which is characteristically hypervascularized by a dense and specialized capillary network and high levels of vascular endothelial growth factor (8). These characteristics provide opportunities for the therapeutic use of anti-angiogenesis agents (9).

Surufatinib is a novel oral tyrosine kinase inhibitor that simultaneously targets angiogenesis [vascular endothelial growth factor receptor and tumor-immune evasion (colony-stimulating factor-1 receptor)]. In the randomized placebo-controlled phase III trial, SANET-p, surufatinib demonstrated a prolonged median progression-free survival (PFS) than placebo [10.9 *vs.* 3.7 months; hazard ratio (HR)=0.49, 95% confidence interval (95% CI): 0.32–0.76; P=0.001], indicating its clinical benefits for pancreatic NET (pNET) (10). Notably, PNELM accounted for 94.2% of the SANET-p population, hinting at the potential strong impact of surufatinib on a subgroup of patients with LM.

Contrast-enhanced computed tomography (CECT) is widely used for the diagnosis and evaluation of treatment responses in cancer patients (11-13). Pre-treatment radiological evaluation may have considerable clinical implications for identifying optimal subgroups. Radiology-based prognosis stratification has demonstrated the association between blood-supply-related imaging features and treatment efficacy (12). By using more quantitative and precise approaches, pre-treatment imaging has become a convenient method for predicting the prognosis and efficacy (14). High-vascularized lesions, for instance, the PNELM, theoretically had the future. They would most benefit treatment with anti-angiogenic therapy (15). Surufatinib, an efficacious angiogenic therapy, may also benefit from this approach.

This study aimed to investigate the association between qualitative and quantitative radiological parameters and the prognosis and efficacy of PNELM treated with surufatinib, hoping to optimize an effective therapy strategy for subgroups of patients receiving surufatinib treatment.

Materials and methods

Patient selection and eligibility

The analysis was conducted in all patients with PNELM from SANET-p, a multicenter, randomized controlled phase III trial. SANET-p was conducted in accordance

with good clinical practice principles and relevant local regulations. Pathology was reviewed and diagnosis was confirmed by two independent pathologists according to the 2019 5th edition of the World Health Organization (WHO) Classification of Neuroendocrine Tumors. Clinical information was retrieved using the hospital information system. The basic eligibility criteria mainly complied with the trial. Key inclusion criteria in this analysis included: 1) above 18 years old; 2) pathological diagnosis of unresectable or metastatic, well differentiated pancreatic NETs (pathological grade 1 or 2 according to the 2010 WHO classification); 3) Eastern Cooperative Oncology Group performance status <2; 4) CECT completed within 4 weeks before the first dose of surufatinib; 5) estimated survival of more than 3 months; and 6) at least one dose of surufatinib or placebo. Key exclusion criteria mainly included: 1) no confirmed liver lesions or no measurable lesions (diameter <1 cm) (n=12); 2) no CECT assessment at baseline (n=3); or 3) images could not be analyzed because of artifacts. All subjects gave written informed consent and the study protocol was approved by the institutional review committee of Peking University Cancer Hospital according to the Helsinki Declaration.

CT technique and assessment criteria

All patients received pre-treatment CECT of the abdomen (liver dual phase) and pelvis, with the scanning coverage ranging from the dome of the right diaphragm to the symphysis pubis or lower according to the standard scanning protocol (the tube voltage was 120 kVp and current was 200 mA). The intravenous administration of 100−150 mL (150−300 mg/mL) of nonionic contrast material at a rate of 2−3 mL/s was required. Images were acquired first for the arterial phase and subsequently for the portal venous phase. The slice thickness was 5 mm with no slice gap, and followed by contiguous reconstruction increments of 5 mm. The image acquisition guideline (*Supplementary Table S1*) was followed by all centers involved in the SANET-p trial. All pre-treatment and subsequent CECT data were retrieved in a workstation (picture archiving and communication system, PACS) for further assessment. Evaluation of CECT images was performed by two qualified radiologists, and when inconsistencies occurred, the assessment was arbitrated by an independent third member. All the imaging reviewers were blinded to the clinical information.

Target liver metastatic lesions according to Response Evaluation Criteria in Solid Tumors (RECIST) version 1.1 were selected from baseline CECT images, avoiding blood vessels and normal liver parenchyma. The region of interest (ROI) was delineated manually in the arterial phase. The ROI were traced along the outer margin of the metastatic tumor of each slice to contain the whole lesion. Subsequently, the CT values of each region were measured in HU on the workstation ($HUtumor_{ART}$). ROI was then measured at the periphery of the lesion and at the maximum slice to record the parameter-peri (parameters are described below). The parameter-whole was measured as the averaged values of the peripheral area and central area (except for obvious necrotic areas in cores). $HUliver_{ART}$ and aorta ($HUaorta_{ART}$) were measured. Finally, HUtumor, HUliver, and HUaorta were measured in non-enhanced and $HUtumor_{PORT}$, $HUliver_{PORT}$ were obtained in portal venous phase slice target lesions.

Imaging parameters

The radiologic features involved qualitative and quantitative parameters. The qualitative parameters included the total hepatic lesion volume (<25% *vs.* ≥25%) (16), hepatic tumor localization type classified by Frilling *et al.* [single metastasis (type I), isolated metastatic bulk accompanied by smaller deposits (type II), disseminated metastatic spread (type III)] (3), tumor margins (poorly-defined or well-defined), enhancement pattern [high enhancement and other (including low enhancement and heterogeneous enhancement) patterns], and necrosis proportions of lesions (≤25% *vs.* >25%) (17).

Quantitative parameters were mainly set as ratios between the tumor tissues and reference vessels, to avoid the inevitable variability between examinations and patients (18). Quantitative parameters included:

(a) Maximum diameter (MD) was defined as the longest diameter of the maximum lesion, measured by the longest transverse diameter axially in slices.

(b) Relative enhancement ratio (RER) was defined as the tumor density compared to the adjacent parenchyma in arterial ($HUtumor_{ART}$/HUliver, ARER) or portal venous phases ($HUtumor_{PORT}$/HUliver, PRER). The RER-peri and RER-whole were calculated depending on the specific position of the lesions (19,20).

(c) Standardized enhancement ratio (SER) was defined as the tumor density compared with aortic enhancement ($HUtumor_{ART}$/HUaorta, ASER) of the arterial phase and portal phase, and portal enhancement ($HUtumor_{PORT}$/HUaorta, PSER). The SER-peri and RER-whole were calculated depending on the specific position of the lesions (20,21).

Efficacy assessment

Patients were re-assessed by investigators using consistent imaging evaluating methods per RECIST version 1.1 every 8 weeks (±3 d) for the first 12 months and then every 12 weeks (±3 d) until progression disease (PD). SANET-p was performed in parallel by the investigators and blinded independent image review committee for efficacy analysis in SANET-p (10). Efficacy variables in the analysis included: the primary end point was defined as the time from randomization to documented PD or death, and the median PFS was the time taken for half of the patients to reach the primary end point. The objective response (OR) was defined as a complete response (CR) or partial response (PR). The disease control rate (DCR) was defined as the proportion of patients with CR, PR, or stable disease (SD).

Statistical analysis

Continuous variables were tested by the *t*-test (normally distributed variables), and categorical variables were compared using Chi-square test or Fisher's exact test, where appropriate. We generated PFS curves using the Kaplan-Meier method and log-rank test. Forest plots depicting the PFS of subgroups were presented. The quantitative radiological parameters were stratified below and above the 50th percentile as low or high levels (e.g. ASER-peri low or high). To assess the association between PFS and the prognostic value of different radiological parameters, multivariate analysis following univariate analysis was conducted using Cox's proportional hazards model. Logistical regressions with univariate/multivariate analysis were performed to evaluate the efficacy. Statistical significance was set at $P<0.05$. All analyses were performed with SAS Enterprise® (Version 8.2; Cary, NC, USA).

Results

Overview of whole cohort

Among 172 patients in the SANET-p trial, patients with no confirmed liver lesions or no measurable lesions (n=12); no CECT assessment at baseline (n=3); and inadequate images for analysis (n=5) were excluded according to the eligibility criteria. We included 152 patients [surufatinib (n=100) and placebo (n=52)] diagnosed with PNELM, who had baseline and at least one post baseline CECT evaluation from the SANET-p study. The flowchart illustrating the exclusion process is shown in *Supplementary Figure S1*. In the surufatinib group, the overall median (range) age was 50.0 (25.0–75.0) years and 87% patients were G2. Baseline characteristics were balanced between the surufatinib and placebo groups (*Table 1*). The radiological deciphering of enhancement and margin-related features are shown in *Supplementary Figure S2* and *Figure 1*.

The summary of imaging parameters is listed in *Supplementary Table S2*. In the surufatinib group, 56 (56.0%) and 44 (44.0%) patients had well- or poorly-defined tumor margins, respectively. Thirty-two patients (32.0%) had high enhancement pattern, mean [standard deviation (SD)] of ASER-peri and ASER-whole was 0.46 (0.15), and 0.38 (0.14); mean (SD) of PSER-peri and PSER-whole was 0.80 (0.14), and 0.69 (0.15); and mean (SD) of ARER-peri and ARER-whole was 1.51 (0.97) and 1.27 (0.90); mean (SD) of PRER-peri and ARER-whole was 1.11 (0.34) and 0.95 (0.31), respectively. No major differences in baseline imaging features were observed between the surufatinib and placebo groups.

Efficacy analysis of whole cohort

The PFS was 11.0 months in the surufatinib group compared to 3.7 months in the placebo group, with an HR of 0.44 (95% CI, 0.29–0.68), indicating a 56% reduction in the risk of disease progression with surufatinib (*Figure 2*). Subgroup analyses of PFS consistently demonstrated benefit across most imaging parameters in the PNELM population, with no suggested influence of baseline covariates on PFS (*Supplementary Table S3*).

Notably, a significant reduction in PFS events was observed in subgroups defined by blood-supply-associated imaging parameters (HR<0.4), including high enhancement pattern, well-defined tumor margins, type III localization metastases, high MDs, necrosis proportions >25%, and hepatic tumor volume <25%.

In terms of response, the surufatinib group demonstrated a best overall response (BOR) of PR in 20 (20.0%) patients, SD in 60 (60.0%) patients, PD in 7 (7.0%) patients, and not evaluable (NE) in 13 (13.0%) patients. In comparison, the placebo group had a BOR of PR in 1 (1.9%) patient, SD in 30 (57.7%) patients, PD in 14 (26.9%) patients, and NE in 7 (13.5%) patients. The objective response ratio (ORR) was 20.0% in the surufatinib group and 1.9% in the placebo group. The ORR results were consistent with those observed in the SANET-p study (*Supplementary Table S4*).

Efficacy analysis of surufatinib group

Further exploration of qualitative and quantitative enhancement parameters and efficacy in the surufatinib

Table 1 Baseline clinical information of surufatinib *vs.* placebo in SANET-p of whole cohort

Variables	n (%)		
	Surufatinib group (N=100)	Placebo group (N=52)	Total
Age (year)			
Median (IQR)	50.0 (43.5–57.0)	48.0 (41.0–60.0)	49.5 (43.0–57.0)
Range	25.0–75.0	20.0–77.0	20.0–77.0
Sex			
Female	48 (48)	28 (54)	76 (50)
Male	52 (52)	24 (46)	76 (50)
ECOG performance status			
0	65 (65)	39 (75)	104 (68)
1	35 (35)	13 (25)	48 (32)
WHO pathological grade			
G1	13 (13)	5 (10)	18 (12)
G2	87 (87)	47 (90)	134 (88)
Proliferation marker protein Ki-67 index			
<5%	36 (36)	15 (29)	51 (34)
5%–10%	50 (50)	30 (58)	80 (53)
>10%	14 (14)	7 (13)	21 (14)
Functional status			
Functioning	9 (9)	3 (6)	12 (8)
Non-functioning	91 (91)	48 (92)	139 (91)
Unknown	0 (0)	1 (2)	1 (1)
Extra-hepatic metastatic sites			
Lymph nodes	35 (35)	18 (35)	53 (35)
Lung	7 (7)	2 (4)	9 (6)
Bone	12 (12)	1 (2)	13 (9)
Other	21 (21)	5 (10)	26 (17)
No. of organs involved			
≤2	46 (46)	30 (58)	76 (50)
>2	54 (54)	22 (42)	76 (50)
Previous-line systemic anti-tumor drug			
Any previous systemic anti-tumor treatment	65 (65)	36 (69)	101 (66)
Previous somatostatin analogue treatment	41 (41)	28 (54)	69 (45)
Previous systemic chemotherapy	29 (29)	10 (19)	39 (26)
Previous everolimus treatment	11 (11)	3 (6)	14 (9)
Previous anti-angiogenic treatment	5 (5)	6 (12)	11 (7)
Sunitinib	4 (4)	6 (12)	10 (7)
Endostatin	1 (1)	1 (2)	2 (1)
Famitinib	1 (1)	0 (0)	1 (1)
Apatinib	0 (0)	1 (2)	1 (1)
Surgery history of primary tumor			
Yes	40 (40)	27 (52)	67 (45)
No	60 (60)	25 (48)	85 (55)

IQR, interquartile range; ECOG, Eastern Cooperative Oncology Group.

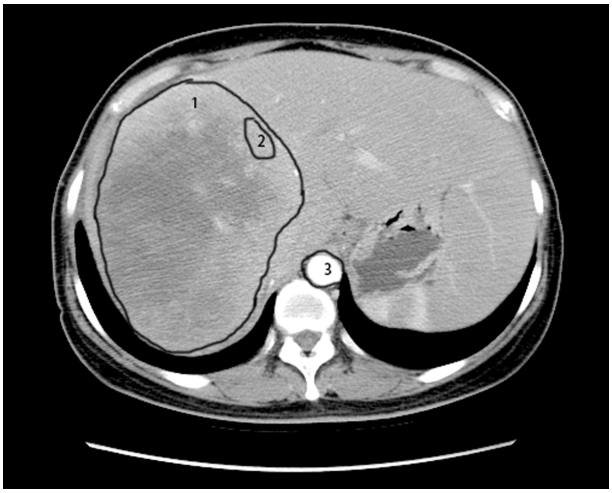

Figure 1 Delineation of target lesions and ROIs. ROI (number 1) was depicted along the contours of the tumor and the average of CT values was calculated as the whole-lesion values. In addition, the ROI (number 2) was generated on the periphery of the tumor; while the ROI (number 3) inside the aorta was depicted to calculate the peri-lesion values. ROI, region of interest; CT, computed tomography.

group revealed potential predictive factors for longer mPFS using univariate Cox regression analysis: high ASER-peri (HR=0.094, 95% CI: 0.009–0.931, P=0.043), low PRER-whole (HR=2.080, 95% CI: 0.881–4.908, P=0.095), and low PRER-peri (HR=2.051, 95% CI: 0.959–4.388, P=0.064). Proceeding with the multivariate analysis, ASER-peri (HR=0.039, 95% CI: 0.003–0.483, P=0.012) and PRER-whole (HR=2.872, 95% CI: 1.299–6.348, P=0.009) were significantly associated with PFS (*Table 2*). PFS curves stratified by ASER-peri (low/high) and PRER-whole (low/high) are shown in *Supplementary Figure S3* and *Supplementary Figure S4*. These figures demonstrate that ASER-peri-high is associated with longer mPFS compared to the other groups.

When examining the association between radiological factors and response in the surufatinib group using logistic analysis, we found that a high enhancement pattern was associated with a better ORR [high enhancement pattern *vs.* other enhancement pattern, 31.3% *vs.* 14.7%, OR=3.488 (95% CI: 1.024–11.875), P=0.046]. Well-defined tumor margins also showed a tendency towards better response in the surufatinib group [25.0% *vs.* 13.6%, OR=3.142 (95% CI: 0.808–12.224), P=0.099] (*Table 3*). Furthermore, well-defined tumor margins were associated with a better DCR [89.3% *vs.* 68.2%, OR=4.535 (95% CI: 1.285–16.011), P=0.019] in the multivariate logistic

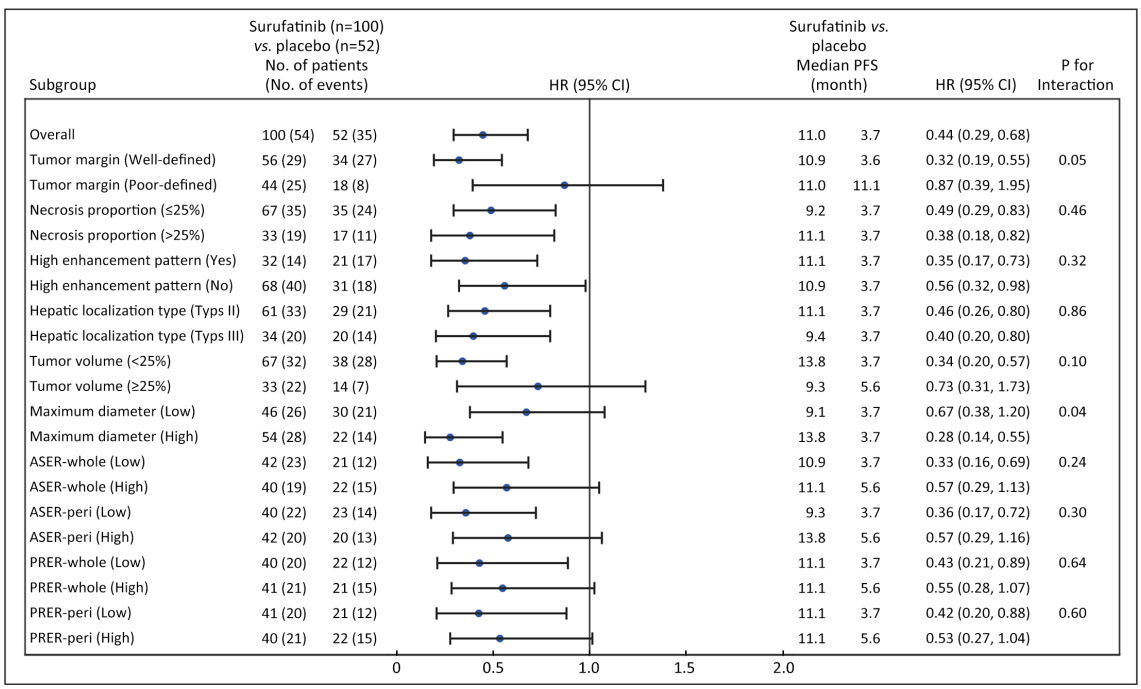

Figure 2 Forest plot of subgroup analysis in imaging characteristics and PFS assessed by the investigators. ASER, arterial standardized enhancement ratio; PRER, portal venous relative enhancement ratio; HR, hazard ratio; 95% CI, 95% confidence interval; PFS, progression-free survival.

Table 2 Cox proportional hazards regression models of variables associated with PFS outcomes in surufatinib

Co-variate	Univariate analysis†			Multivariate analysis		
	HR (95% CI)	P	N	HR (95% CI)	P	N
Tumor margin [Poorly-defined (n=44) *vs.* Well-defined (n=56)]	0.958 (0.560, 1.650)	0.878	100			
Necrosis proportion [>25% (n=33) *vs.* ≤25% (n=67)]	0.690 (0.393, 1.213)	0.198	100			
High enhancement pattern [Others (n=68) *vs.* High (n=32)]	0.940 (0.506, 1.749)	0.846	100			
Tumor volume [≥25% (n=33) *vs.* <25% (n=67)]	1.269 (0.736, 2.187)	0.392	100			
Hepatic localization type			99			
Type II (n=61) *vs.* Type I (n=4)	4.707 (0.640, 34.623)	0.128				
Type III (n=34) *vs.* Type I (n=4)	3.861 (0.516, 28.869)	0.188				
Maximum diameters	0.992 (0.983, 1.002)	0.101	100			
ARER-whole	1.182 (0.875, 1.596)	0.276	82			
ARER-peri	1.153 (0.860, 1.546)	0.341	82			
PRER-whole	2.080 (0.881, 4.908)	0.095	81	2.872 (1.299, 6.348)	0.009	81
PRER-peri	2.051 (0.959, 4.388)	0.064	81			
ASER-whole	0.124 (0.010, 1.514)	0.102	82			
ASER-peri	0.094 (0.009, 0.931)	0.043	82	0.039 (0.003, 0.483)	0.012	81
PSER-whole	1.544 (0.260, 9.182)	0.633	81			
PSER-peri	1.811 (0.297, 11.031)	0.520	81			

†, Patients with evaluable assessment, N=81 (Other patients had uncalculating lesions); Parameters with P<0.1 from univariate analysis entered into the multivariate analysis. Stepwise selection (entry and removal significance level =0.1) was performed to find the best performing model. PFS, progression-free survival; ARER, arterial relative enhancement ratio; PRER, portal venous relative enhancement ratio; ASER, arterial standardized enhancement ratio; PSER, portal venous standard enhancement ratio; HR, hazard ratio; 95% CI, 95% confidence interval. PRER-peri did not enter the final model during the construction of models by stepwise selection (P<0.1).

regression analysis (*Supplementary Table S5*). No differences in ORR/DCR were observed in comparisons with different localization types, tumor volumes, necrosis proportions, and ASER-peri values.

Discussion

Although surufatinib provided significant clinical benefit regarding the PFS of PNELM patients, more precise methods are warranted to distinguish non-beneficiaries. We utilized blood-supply-associated imaging parameters as markers for surufatinib to evaluate its potential in PNELM. The results suggested that high ASER-peri, high enhancement patterns, and well-defined tumor margins could be predictors for better PFS and optimal ORR/DCR in surufatinib-treated patients.

We hypothesized that high blood-supply pre-treatment CECT parameters might correlate with the response to surufatinib, because vascularization positively correlated to efficacy, lesions with high blood supply may provide greater access to anti-angiogenesis agents (surufatinib) as well as markers of tumors with well-developed tumor vessels (9). Some identified radiological predictors, including the pre-treatment enhancement ratio (ER), have already been associated with treatment effectiveness (20,22). Such quantitative indexes have advantages in standardization for precise clinical practice and future research. Studies have mainly focused on enhancement patterns, which had positive relationships with promising objective responses in patients treated with anti-angiogenesis agents (23). Volume of lesion enhancement and tumor micro-vessel density were also significant prognostic factors (21,22,24,25). The baseline CT arterial enhancement pattern/fraction also improved the PFS and response in patients with transcatheter arterial embolization, chemotherapy, radioembolization, or surgery (13,15,19,26-29).

We demonstrated that blood supply-associated radiological features (high ASER-peri and low PRER-whole values) revealed PFS benefit in the surufatinib group, which is applicable for future treatment judgement. Given the necessity to exclude the interference of different

Table 3 Logistic regression of variables associated with ORR in surufatinib groups

Co-variate	Univariate analysis					Multivariate analysis				
	OR	95% CI	P	Type 3 tests	N	OR	95% CI	P	Type 3 tests	N
Tumor margin [Well-defined (n=56) *vs.* poorly-defined (n=44)]	2.110	0.737, 6.061	0.164	0.164	100	3.142	0.808, 12.224	0.099	0.099	82
Necrosis proportion [>25% (n=33) *vs.* ≤25% (n=67)]	1.118	0.399, 3.136	0.832	–	100	–	–	–	–	–
Tumor volume [≥25% (n=33) *vs.* <25% (n=67)]	1.467	0.533, 4.035	0.458	–	100	–	–	–	–	–
High enhancement pattern [High (n=32) *vs.* others (n=68)]	2.636	0.965, 7.199	0.059	0.059	100	3.488	1.024, 11.875	0.046	0.046	82
Hepatic localization type					99					82
Type I (n=4) *vs.* Type III (n=34)	2.400	0.296, 19.485	0.413	0.068		0.517	0.042, 6.413	0.607	0.080	
Type II (n=61) *vs.* Type III (n=34)	0.362	0.127, 1.032	0.057	–		0.222	0.058, 0.849	0.028	–	
ASER-peri	0.752	0.263, 2.150	0.594	0.594	82	0.834	0.255, 2.727	0.764	0.764	82

ORR, objective response ratio; ASER, arterial standardized enhancement ratio; OR, odds ratio; 95% CI, 95% confidence interval. The parameters with P values <0.1 were entered into the multivariate analysis.

scan conditions, we employed standard enhancement ratios. Among these parameters, the peri-lesion enhancement reflecting the blood supply may have similar practical value to whole-lesions. The measurement of central-lesion parameters, however, was inferior to that of peri/whole-lesions (30,31), which may be due to the core of the lesions being filled with necrosis components and introducing some miscalculation. The ASER-peri, thereafter, is affirmed as the ideal precise measurement because it was positively correlated to the blood supply.

Patients with well-defined margins and high enhancement patterns were more likely to have higher ORR (32). We observed the in-concordance of efficacy by imaging markers between ORR and PFS, which might be caused by the imperfect association between the PFS and ORR benefit generated from the slow progression nature of pNET (long duration SD was calculated as PFS benefit, but was not recorded as remission).

Our study had some noteworthy strengths. First, all data were collected from a multicenter double-blinding phase III clinical trial, excluding commonly-seen heterogeneity in retrospective cohorts. Second, we analyzed the data with large samples to increase the reliability. We revealed that ordinary pre-treatment CECT assessments can be extraordinary prognostic parameters for PNELM patients. Furthermore, the major populations were G2 patients, eliminating common pathological confounding factors (13,33,34).

Our study had some limitations. The analysis of CT scans was performed in different centers, which introduced variability in the measurement of parameters. Additionally, subjectivity was present in manual procedures such as defining the ROI on CT images. In the future, artificial intelligence might offer solutions to address these challenges and ensure more consistent and objective measurements (15).

Conclusions

Our study emphasized the association between pre-treatment high blood-supply radiological parameters of tumors and the efficacy of surufatinib in patients with PNELM. Specifically, high ASER-peri emerged as a significant factor that benefited the PFS. Moreover, a high enhancement pattern and well-defined tumor margins were associated with a better ORR and DCR in these challenging cases of refractory PNELM. These pre-treatment CECT characteristics have the potential to enhance patient selection and contribute to improving management strategies for PNELM.

Acknowledgements

None.

Footnote

Conflicts of Interest: Yujie Yang, Haoyun Shi, Xian Luo, Songhua Fan, and Weiguo Su are employees of HUTCHMED Limited and report personal fees from HUTCHMED Limited both during and outside the

conduct of the study. The other authors have no conflicts of interest to declare.

References

1. Dasari A, Shen C, Halperin D, et al. Trends in the incidence, prevalence, and survival outcomes in patients with neuroendocrine tumors in the United States. JAMA Oncol 2017;3:1335-42.
2. Pavel M, O'Toole D, Costa F, et al. ENETS consensus guidelines update for the management of distant metastatic disease of intestinal, pancreatic, bronchial neuroendocrine neoplasms (NEN) and NEN of unknown primary site. Neuroendocrinology 2016;103:172-85.
3. Frilling A, Modlin IM, Kidd M, et al. Recommendations for management of patients with neuroendocrine liver metastases. Lancet Oncol 2014;15:e8-21.
4. Frilling A, Li J, Malamutmann E, et al. Treatment of liver metastases from neuroendocrine tumors in relation to the extent of hepatic disease. Br J Surg 2009;96:175-84.
5. Cloyd JM, Wiseman JT, Pawlik TM. Surgical management of pancreatic neuroendocrine liver metastases. J Gastrointest Oncol 2020;11:590-600.
6. Demirkan BH, Eriksson B. Systemic treatment of neuroendocrine tumors with hepatic metastases. Turk J Gastroenterol 2012;23:427-37.
7. Rinke A, Müller HH, Schade-Brittinger C, et al. Placebo-controlled, double-blind, prospective, randomized study on the effect of octreotide LAR in the control of tumor growth in patients with metastatic neuroendocrine midgut tumors: a report from the PROMID Study Group. J Clin Oncol 2009;27:4656-63.
8. Couvelard A, O'Toole D, Turley H, et al. Microvascular density and hypoxia-inducible factor pathway in pancreatic endocrine tumors: negative correlation of microvascular density and VEGF expression with tumor progression. Br J Cancer 2005;92:94-101.
9. Jain RK. Normalizing tumor vasculature with anti-angiogenic therapy: a new paradigm for combination therapy. Nat Med 2001;7:987-9.
10. Xu J, Shen L, Bai C, et al. Surufatinib in advanced pancreatic neuroendocrine tumors (SANET-p): a randomised, double-blind, placebo-controlled, phase 3 study. Lancet Oncol 2020;21:1489-99.
11. Heneweer C, Holland JP, Divilov V, et al. Magnitude of enhanced permeability and retention effect in tumors with different phenotypes: 89Zr-albumin as a model system. J Nucl Med 2011;52:625-33.
12. Kim KW, Lee JM, Klotz E, et al. Quantitative CT color mapping of the arterial enhancement fraction of the liver to detect hepatocellular carcinoma. Radiology 2009;250:425-34.
13. Cappelli C, Boggi U, Mazzeo S, et al. Contrast enhancement pattern on multidetector CT predicts malignancy in pancreatic endocrine tumors. Eur Radiol 2015;25:751-9.
14. Chen L, Wang W, Jin K, et al. Special issue "the advance of solid tumor research in China": Prediction of sunitinib efficacy using computed tomography in patients with pancreatic neuroendocrine tumors. Int J Cancer 2023;152:90-9.
15. Okabe H, Hashimoto D, Chikamoto A, et al. Shape and enhancement characteristics of pancreatic neuroendocrine tumor on preoperative contrast-enhanced computed tomography may be prognostic indicators. Ann Surg Oncol 2017;24:1399-405.
16. Panzuto F, Pusceddu S, Faggiano A, et al. Prognostic impact of tumor burden in stage IV neuroendocrine neoplasia: A comparison between pancreatic and gastrointestinal localizations. Pancreatology 2019;19:1067-73.
17. Beleù A, Rizzo G, De Robertis R, et al. Liver tumor burden in pancreatic neuroendocrine tumors: CT features and texture analysis in the prediction of tumor grade and ^{18}F-FDG uptake. Cancers (Basel) 2020;12:1486.
18. Gulpinar B, Peker E, Soydal C, et al. Can we differentiate histologic subtypes of neuroendocrine tumor liver metastases at a single phase contrast-enhanced CT-correlation with Ga-68 DOTATATE PET/CT findings. Br J Radiol 2020;93:20190735.
19. D'Onofrio M, Ciaravino V, Cardobi N, et al. CT enhancement and 3D texture analysis of pancreatic neuroendocrine neoplasms. Sci Rep 2019;9:2176.
20. Nagayama Y, Inoue T, Kato Y, et al. Relative enhancement ratio of portal venous phase to unenhanced CT in the diagnosis of lipid-poor adrenal adenomas. Radiology 2021;301:360-8.
21. Liu Y, Chen W, Cui W, et al. Quantitative pretreatment CT parameters as predictors of tumor

response of neuroendocrine tumor liver metastasis to transcatheter arterial bland embolization. Neuroendocrinology 2020;110:697-704.
22. Kawamura Y, Kobayashi M, Shindoh J, et al. Pretreatment heterogeneous enhancement pattern of hepatocellular carcinoma may be a useful new predictor of early response to lenvatinib and overall prognosis. Liver Cancer 2020;9:275-92.
23. Gebauer L, Moltz JH, Mühlberg A, et al. Quantitative imaging biomarkers of the whole liver tumor burden improve survival prediction in metastatic pancreatic cancer. Cancers (Basel) 2021;13:5732.
24. Xu W, Yan H, Xu L, et al. Correlation between radiologic features on contrast-enhanced CT and pathological tumor grades in pancreatic neuroendocrine neoplasms. J Biomed Res 2020;35: 179-88.
25. Colagrande S, Calistri L, Campani C, et al. CT volume of enhancement of disease (VED) can predict the early response to treatment and overall survival in patients with advanced HCC treated with sorafenib. Eur Radiol 2021;31:1608-19.
26. Marrache F, Vullierme MP, Roy C, et al. Arterial phase enhancement and body mass index are predictors of response to chemoembolisation for liver metastases of endocrine tumors. Br J Cancer 2007;96:49-55.
27. Joo I, Lee JM, Kim KW, et al. Liver metastases on quantitative color mapping of the arterial enhancement fraction from multiphasic CT scans: Evaluation of the hemodynamic features and correlation with the chemotherapy response. Eur J Radiol 2011;80:e278-83.
28. Jarraya H, Borde P, Mirabel X, et al. Lobulated enhancement evaluation in the follow-up of liver metastases treated by stereotactic body radiation therapy. Int J Radiat Oncol Biol Phys 2015;92:292-8.
29. Wang Z, Ye Y, Hu Y, et al. Extent of enhancement on multiphase contrast-enhanced CT images is a potential prognostic factor of stage I-III colon cancer. Eur Radiol 2019;29:1114-23.
30. Zhu HB, Xu D, Zhang XY, et al. Prediction of therapeutic effect to treatment in patients with colorectal liver metastases using functional magnetic resonance imaging and RECIST criteria: A pilot study in comparison between bevacizumab-containing chemotherapy and standard chemotherapy. Ann Surg Oncol 2022;29:3938-49.
31. Sun YQ, Xiao Q, Hu FX, et al. Diffusion kurtosis imaging in the characterisation of rectal cancer: utilizing the most repeatable region-of-interest strategy for diffusion parameters on a 3T scanner. Eur Radiol 2018;28:5211-20.
32. Froelich MF, Heinemann V, Sommer WH, et al. CT attenuation of liver metastases before targeted therapy is a prognostic factor of overall survival in colorectal cancer patients. Results from the randomised, open-label FIRE-3/AIO KRK0306 trial. Eur Radiol 2018;28:5284-92.
33. Kim DW, Kim HJ, Kim KW, et al. Neuroendocrine neoplasms of the pancreas at dynamic enhanced CT: comparison between grade 3 neuroendocrine carcinoma and grade 1/2 neuroendocrine tumour. Eur Radiol 2015;25:1375-83.
34. Belousova E, Karmazanovsky G, Kriger A, et al. Contrast-enhanced MDCT in patients with pancreatic neuroendocrine tumors: correlation with histological findings and diagnostic performance in differentiation between tumour grades. Clin Radiol 2017;72:150-8.

Cite this article as: Zhang J, Zhu H, Shen L, Li J, Zhang X, Bai C, Zhou Z, Yu X, Li Z, Li E, Yuan X, Lou W, Chi Y, Xu N, Yin Y, Bai Y, Zhang T, Xiu D, Chen J, Qin S, Wang X, Yang Y, Shi H, Luo X, Fan S, Su W, Lu M, Xu J. Baseline radiologic features as predictors of efficacy in patients with pancreatic neuroendocrine tumors with liver metastases receiving surufatinib. Chin J Cancer Res 2023;35(5):526-535. doi: 10.21147/j.issn.1000-9604.2023.05.09

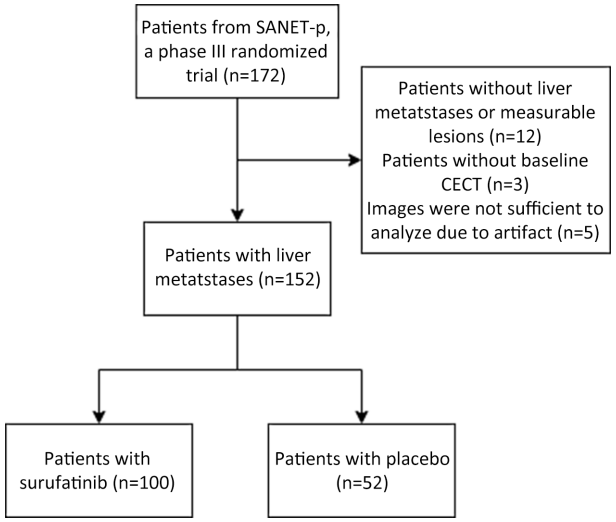

Figure S1 Flowchart of the study. CECT, contrast-enhanced computed tomography.

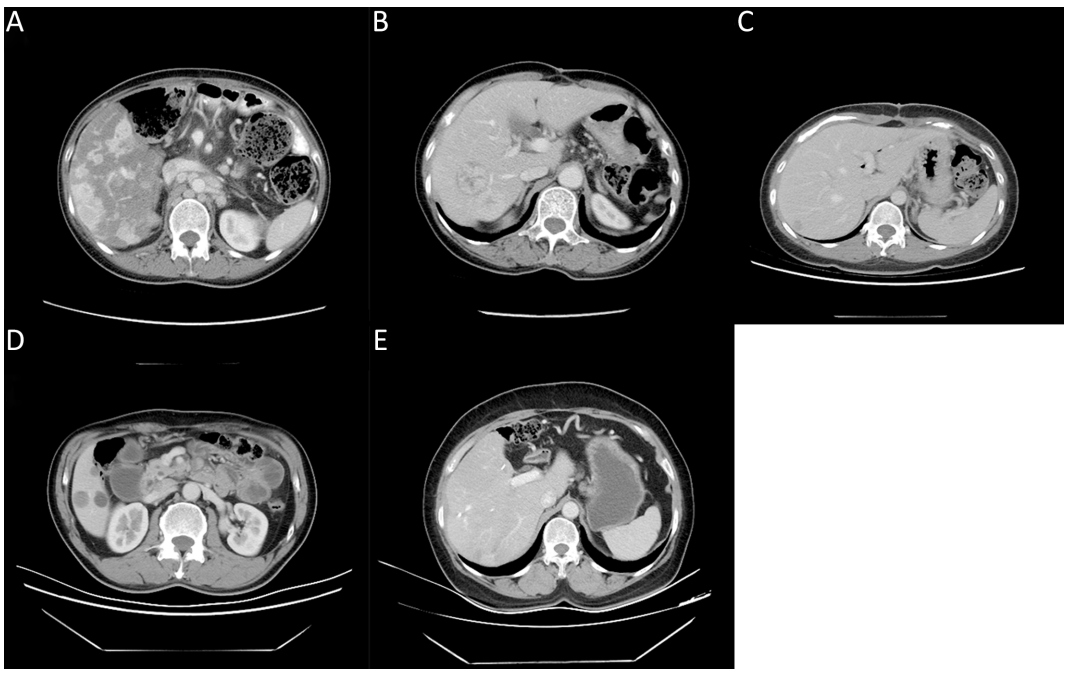

Figure S2 Examples of some radiological features seen on pre-treatment CECT of qualitative enhancement measurements. (A) Low enhancement; (B) High enhancement; (C) Heterogeneous enhancement; (D) Well-defined margins; (E) Poorly-defined margins. CECT, contrast-enhanced computed tomography.

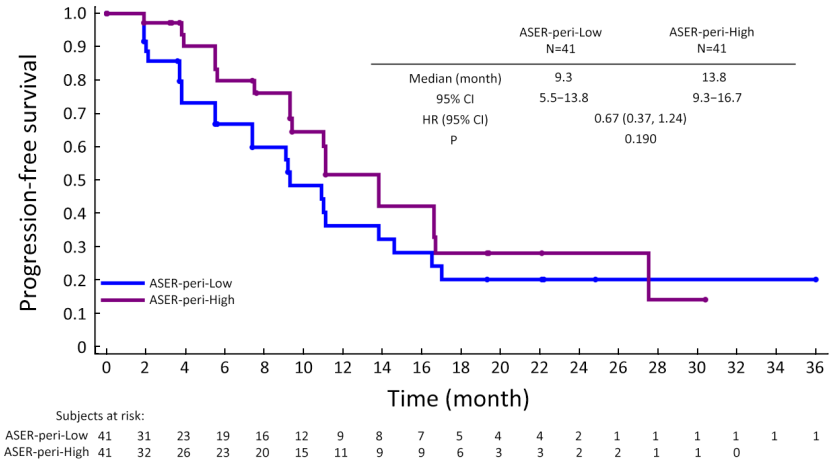

Figure S3 Kaplan-Meier plot showing PFS according to ASER-peri extent (high *vs.* low). PFS, progression-free survival; ASER, arterial standardized enhancement ratio; HR, hazard ratio; 95% CI, 95% confidence interval.

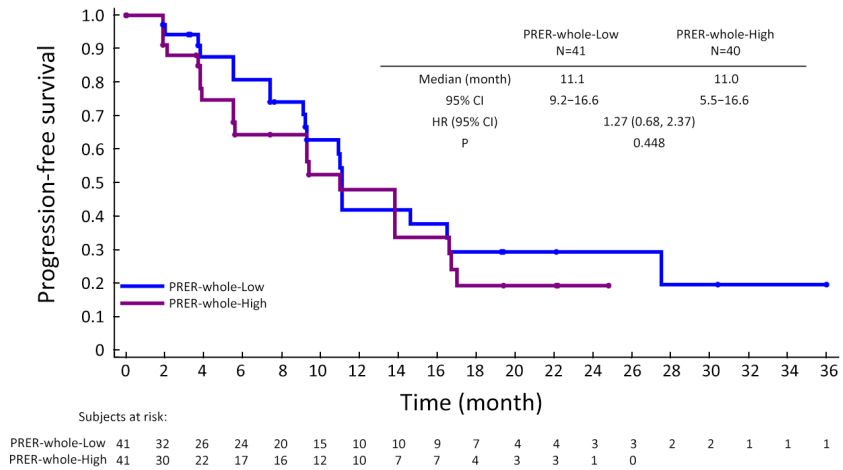

Figure S4 Kaplan-Meier plot showing PFS according to PRER-whole extent (high *vs.* low). PFS, progression-free survival; PRER, portal venous relative enhancement ratio; HR, hazard ratio; 95% CI, 95% confidence interval.

Table S1 CT scanning protocol in the study

Variables	SCAN1	SCAN2	SCAN3
Scan phase/delay	Pre-contrast	Ensure high-quality imaging of the liver	
		Arterial phase	Portal phase
Scan location/coverage	Dome of the right diaphragm through the symphysis pubis or lower to ensure complete coverage of the pelvis	Lung apices through entire liver	Dome of the right diaphragm through the symphysis pubis or lower to ensure complete coverage of the pelvis
Patient orientation	Supine	Supine	Supine
Breathing instruction	Abdomen and pelvis performed in one breath-hold	Chest and entire liver performed in one breath-hold	Abdomen and pelvis in one breath-hold
Scan FOV	Large	Large	Large
Display FOV	Unique to patient size	Unique to patient size	Unique to patient size
Slice thickness	5 mm	5 mm	5 mm
Reconstruction interval	5 mm	5 mm	5 mm
Gap (slice spacing)	None (i.e. contiguous)	None (i.e. contiguous)	None (i.e. contiguous)
Contrast media instructions			
i.v. contrast	Required 100–150 mL non-ionic only	Required 100–150 mL non-ionic only	Required 100–150 mL non-ionic only
i.v. contrast concentration	150–300 mg/mL	150–300 mg/mL	150–300 mg/mL
Injection rate	Single injection: 2–3 cc/sec (power injector preferred)	Single injection: 2–3 cc/sec (power injector preferred)	Single injection: 2–3 cc/sec (power injector preferred)
Oral contrast	Required (use standard protocol)	Required (use standard protocol)	Required (use standard protocol)

CT, computed tomography; FOV, field of view.

Table S2 Baseline qualitative and quantitative radiological information of surufatinib *vs.* placebo

Level	Overall	Surufatinib	Placebo	P*
Qualitative parameters [n (%)]				
Tumor margin				0.264
Well-defined	90 (59.21)	56 (56.00)	34 (65.38)	
Poorly-defined	62 (40.79)	44 (44.00)	18 (34.62)	
Necrosis proportion				0.144
0–25%	102 (67.11)	67 (67.00)	35 (67.31)	
>25%	50 (32.89)	33 (33.00)	17 (32.69)	
High enhancement pattern				0.370
High	53 (34.87)	32 (32.00)	21 (40.38)	
Not high	99 (65.13)	68 (68.00)	31 (59.62)	
Hepatic localization type				0.727 (exact)
Type I	7 (4.64)	4 (4.04)	3 (5.77)	
Type II	90 (59.60)	61 (61.62)	29 (55.77)	
Type III	54 (35.76)	34 (34.34)	20 (38.46)	
Tumor volume				0.442
≤25%	105 (69.08)	67 (67.00)	38 (73.08)	
>25%	47 (30.92)	33 (33.00)	14 (26.92)	
Quantitative parameters [Mean (SD)]				
Maximum diameters	41.7 (28.84)	44.4 (30.20)	36.7 (25.57)	0.121
ARER-whole	1.31 (0.87)	1.27 (0.90)	1.39 (0.82)	0.467
ARER-peri	1.54 (0.94)	1.51 (0.97)	1.60 (0.87)	0.619
PRER-whole	0.96 (0.29)	0.95 (0.31)	0.98 (0.25)	0.592
PRER-peri	1.12 (0.32)	1.11 (0.34)	1.13 (0.28)	0.658
ASER-whole	0.38 (0.13)	0.38 (0.14)	0.37 (0.11)	0.536
ASER-peri	0.44 (0.15)	0.46 (0.15)	0.42 (0.13)	0.271
PSER-whole	0.69 (0.14)	0.69 (0.15)	0.69 (0.14)	0.909
PSER-peri	0.80 (0.14)	0.80 (0.14)	0.80 (0.15)	0.999
AEI	5.44 (9.43)	5.91 (10.81)	4.58 (6.18)	0.421
PEI	1.67 (0.97)	1.75 (1.11)	1.52 (0.65)	0.156

ARER/PRER, arterial phase/portal venous phase relative enhancement ratio; ASER/PSER, arterial phase/portal venous phase standard enhancement ratio; AEI, arterial enhancement index; PEI, portal-venous enhancement index. *, Continuous variables were tested by the *t*-test (normally distributed variables), and categorical variables were compared using Chi-square test or Fisher's exact test, where appropriate.

Table S3 Univariate analysis of PFS by investigator considering potential influence of baseline covariates

Variables	Subsets (n/n)	HR	95% CI	P
Treatment (Surufatinib/Placebo)	100/52	0.444	0.29, 0.68	<0.001
NET pathological grade (Grade 1/Grade 2)	18/134	0.882	0.44, 1.76	0.722
ECOG performance status (0/1)	104/48	0.724	0.46, 1.14	0.162
Age (year) (<65/≥65)	135/17	0.814	0.43, 1.53	0.523
Gender (Male/Female)	76/76	1.402	0.92, 2.14	0.119
Functioning tumor (Yes/No)	12/139	–	–	–
No. of organs involved by tumor (≤2/≥3)	76/76	0.783	0.51, 1.20	0.257
Prior systemic chemotherapy (Yes/No)	39/113	0.930	0.57, 1.52	0.772
Previous systemic anti-tumor drug for advanced disease (Yes/No)	101/51	1.252	0.80, 1.95	0.321
Prior anti-angiogenesis treatment (Yes/No)	11/141	–	–	–

PFS, progression-free survival; NET, neuroendocrine tumor; ECOG, Eastern Cooperative Oncology Group; HR, hazard ratio; 95% CI, 95% confidence interval. The second level is the reference level for interpretation of HRs for categorical characteristics. If <10% of patients are assigned to a particular stratum, those particular covariates are not included in the analysis.

Table S4 Objective responses in patients of surufatinib cohort

Variables	n/N		P	n/N		P
	ORR	Non-ORR		DCR	Non-DCR	
Tumor margin			0.159			–
Well-defined	14/56	42/56		–	–	
Poorly-defined	6/44	38/44		–	–	
Necrosis proportion			0.832			0.440 (Exact)
0–25%	13/67	54/67		52/67	15/67	
>25%	7/33	26/33		28/33	5/33	
High enhancement pattern			0.054			0.830
No	10/68	58/68		54/68	14/68	
Yes	10/32	22/32		26/32	6/32	
Hepatic metastases localization type			0.048 (Exact)			0.459 (Exact)
Type I	2/4	2/4		4/4	0/4	
Type II	8/61	53/61		47/61	14/61	
Type III	10/34	24/34		29/34	5/34	
Tumor volume			0.457			0.832
<25%	12/67	55/67		54/67	13/67	
≥25%	8/33	25/33		26/33	7/33	
ASER-peri			0.594			0.414
Low	8/41	33/41		31/41	10/41	
High	10/41	31/41		34/41	7/41	
Maximum diameter			0.617			0.617
Low	9/50	41/50		39/50	11/50	
High	11/50	39/50		41/50	9/50	

Parameters with P<0.1 were entered into the multivariate analysis. ASER, arterial standardized enhancement ratio; ORR, objective response ratio; DCR, disease control rate.

Table S5 Logistic regression models of variables associated with DCR of surufatinib cohort

Level	Univariate analysis				Multivariate analysis			
	OR	95% CI	P	Type 3 tests	OR	95% CI	P	Type 3 tests
Tumor margin (Poorly-defined *vs.* well-defined)	0.257	0.089, 0.741	0.012	0.012	4.535	1.285, 16.011	0.019	0.019
Necrosis proportion (>25% *vs.* ≤25%)	1.615	0.532, 4.909	0.398		–	–	–	–
Tumor volume (≥25% *vs.* <25%)	0.894	0.319, 2.507	0.832		–	–	–	–
High enhancement pattern (High *vs.* others)	1.123	0.387, 3.258	0.830	0.830	0.887	0.226, 3.487	0.864	0.864
Hepatic localization type								
Type I *vs.* Type III	–	–	0.981	0.633	–	–	0.982	0.315
Type II *vs.* Type III	0.579	0.189, 1.776	0.339		0.358	0.095, 1.347	0.129	
ASER-peri	0.568	0.013, 24.404	0.769		–	–	–	–

DCR, disease control rate; ASER-peri, arterial standard enhancement rate-peri; OR, odds ratio; 95% CI, 95% confidence interval. No patients with surufatinib with type I hepatic metastases localization types had objective response, thus DCR cannot be estimated.